Journal of Applied Polymer Science

Fabrication and characterization of double-network agarose/polyacrylamide nanofibers by electrospinning

Min Kyoung Cho,[1*] Bal Sydulu Singu,[1*] Yang Ho Na,[2] Kuk Ro Yoon[1]

[1]Department of Chemistry, Hannam University, 461-6 Jeonmin-Dong, Yuseong-Gu, Daejeon 305-811, Korea

[2]Department of Advanced Materials, Hannam University, 461-6 Jeonmin-Dong, Yuseong-Gu, Daejeon 305-811, Korea

Min Kyoung Cho and Bal Sydulu Singu contributed equally to this work.

Correspondence to: K. R. Yoon (E-mail: kryoon@hnu.kr) and Y. H. Na (E-mail: yhna@hnu.kr)

ABSTRACT: This study focused on the preparation of electrospun cross-linked double-network (DN) of agarose/polyacrylamide (PAAm) nanofibers. The agarose formed the first-network that was physical-linked by the agar helix bundles. After UV-irradiation, the chemically crosslinked PAAm was formed as the second network. The resulting cross-linked DN agarose/PAAm nanofibers were characterized by scanning electron microscopy (SEM), contact angle, attenuated total reflectance-Fourier transform infrared spectroscopy (ATR-FT-IR), thermogravimetric analysis (TGA), and tensile test. SEM analysis shows the agarose/PAAM nanofibers present with the thickness of 187 nm. Agarose/PAAm nanofibers were showing FT-IR spectral peaks at ~1660, 1590, and 1070 cm^{-1} indicating the presence of both agarose and polyacrylamide in the crosslinked DN Agarose/PAAm nanofiber sheet, it suggests the strong interaction and good compatibility between the two components. Agarose/PAAm nanofiber sheet was showing thermal stability close to the pure polyacrylamide. From the tensile test study, agarose/PAAm strength improved by 66.66% compared to the pure agarose.
 J. Appl. Polym. Sci. **2016**, *133*, 42914.

KEYWORDS: biomedical applications; electrospinning; fibers; mechanical properties; photopolymerization

Received 3 April 2015; accepted 5 September 2015

DOI: 10.1002/app.42914

INTRODUCTION

To combine PAAm and agarose and complement each other, we introduce a double network (DN) system. The DN possess properties are the combination of agarose and polyacrylamide two networks such as network density, rigidity, molecular weight, crosslinking density, etc. The mechanical properties of DN prepared from many different polymer pairs were shown to be much better than that of the individual components. DN works are usually synthesized via a multistep sequential free radical polymerization process.[1]

Photochemically induced polymerization reactions have become of great importance in industry. The traditional applications of UV-curable systems are in the industrial areas where temperature-sensitive substrates are coated, like wood, paper, varnishes, and plastics and to produce the high-definition images required in the manufacture of microcircuits and printing plates. Photocuring of thin films, such as, for example, in the curing of paint coatings and plastic coatings on paper, wood, metal, and plastic or in the drying of printing inks. This curing by irradiation in the presence of photoinitiators is distinguished, compared with conventional methods for the drying or curing of coatings, by saving of materials and energy, low thermal stress of the substrate, and in particular a high curing rate. Moreover, the preparation of polymer materials by polymerization of the corresponding unsaturated monomeric starting materials is often carried out photochemically and by means of photoinitiators.

The goal of the study is to develop cross linked composite nanofibers with high surface area combined by excellent mechanical and solvent-resistant properties through UV irritations used as biomimetic materials for their potential applications in tissue engineering scaffolds and drug delivery. Ultraviolet (UV) irradiation[2,3] have been employed to crosslink PEO in order to prevent the dissolution and flow of PEO into the external medium. Among the many crosslinking methods, UV-induced crosslinking method exhibits many advantages including easy manipulation, low hazard for the researchers, highly effective and controllable reaction.[4,5] More importantly, the sterilization and crosslinking could be conducted simultaneously during the UV irradiation, which greatly facilitates the utilization of UV-induced crosslinking techniques for biomaterial preparations.

Polyacrylamide (PAAm), prepared by copolymerization of one or more functional monomers with acrylamide (AAm) in the

presence of a crosslinker such as *N,N*-methylenebisacrylamide (MBAA). PAAm have been of great interest due to its applications in horticultural and agriculture,[6] drilling fluids,[7] tissue engineering,[8,9] and waste treatments as a flocculent to bind heavy metal ions by forming coordination bonds.[10,11] Polyacrylamide is often used in molecular biology applications as a medium for electrophoresis of proteins and nucleic acids. These are ascribed to their nontoxic and biologically inertness, long chain length, capacity for preserving their shape and mechanical strength and convenient adjustability of mechanical, chemical, and biophysical properties. Poor mechanical properties have limited further development of PAAm.[12,13] Agarose, a natural polysaccharide obtained from red algae, is a linear polymer made up of the repeating unit of agarobiose, which is a disaccharide made up of D-galactose and 3,6-anhydro-L-galactopyranose unit. It has been extensively used in food and cosmetic industries for a hundred years.[14] During the last few decades, various forms of the agarose-based systems have been developed for the applications in pharmaceutical industries and medical research.[15]

Electrospun polyvinyl alchol/chitosan (PVA/CS) and polyvinylalchol/cyanobacterial extracellular polymeric substances (PVA/EPS) blend nanofibers have been successfully prepared by Carla *et al.*[16] Blend nanofibres showing uniform morphology with a narrow diameter distribution from about 50 to 130 nm are obtained. Dynamic mechanical analysis and filtration test demonstrated that the PVA/EPS electrospun blended membrane has better tensile mechanical properties and resisted more against disintegration in the temperature range between 10 and 50°C. The chitosan/sericin/poly(vinyl alcohol) (CS/SS/PVA) nanofibers incorporated with *in situ* synthesis of nano silver are successfully produced through electrospinning. The obtained Cs/SS/PVA nanofibers are with mean diameter of 180 nm. Introducing $AgNO_3$ not only produces excellent antibacterial activity, but also decreases the Cs/SS/PVA/$AgNO_3$ nanofiber diameter to about 95 nm.[17] Silver nanoparticles/poly (vinyl alcohol) (PVA)/carboxymethyl-chitosan (CM-chitosan) (AgNPs/PVA/CM-chitosan) nanofibers are successfully fabricated by electrospinning. The AgNPs can be observed on the surface of the fibers with round shape, which mainly distributed from 4 to 14 nm in the nanofibers. The comprehensive results of this study suggest that AgNPs/PVA/CM-chitosan nanofibers have the potential to be utilized as antibacterial biomaterials.[18] Non-woven mats of polyvinyl alcohol/chitosan (PVA/CS) blends and PVA/CS blends containing 1 wt % Ag nanoparticles are successfully fabricated by the electrospinning method. The antibacterial experiment indicated that the nonwoven mats of PVA/CS blends have good bactericidal activity against the gram-negative bacteria *E. coli*. The antibacterial activity of nonwoven mats of Ag/PVA/CS blends is better than that of nonwoven mats of PVA/CS blends.[19] Electrospun chitosan/polyacrylamide (CS/PAAm) nanofibers crosslinked with glutaraldehyde vapour had adsorption capacity for Cr(VI) and PO_3^{-4} of 0.26 and 392.00 mg g^{-1}, respectively. The removal efficiencies are 93.0 and 97.4% for Cr(VI) and PO_3^{-4}, respectively.[20] Zhou *et al.*[21] prepared the fibrous hydrolyzed polyacrylamide/cellulose (HPAM/CNC) nanocrystals. HPAM/CNC nanocomposite membranes consist of electrospun fibers with an average diameter of ~220 nm. The porous nanocomposite gels displayed a rapid swelling rate and high adsorption capacity in removing methylene blue from aqueous solution. The novel porous nanocomposite gels show promise as sorbents in the removal of small ionic contaminants from wastewater.

The simple straightforward electrospinning is rapidly developing along two directions, one is the direct creation of structural nanofibers using multiple-fluid electrospinning[22,23] and other one is combined usage of electrospinning with other techniques.[24] The present study demonstrates a preliminary research on the preparation of agarose/PAAm nano fibers by electrospinning followed by photo-polymerization (combined usage of electrospinning and photopolymerization method). It is considered that the present study may increase the versatility of agarose/PAAm nanofibers in terms of the biomedical and bioengineering applications and improvement in mechanical properties, thermal stability, and solvent resistance.

EXPERIMENTAL

Materials

Agarose E (Laboratorios, Conda), acrylamide (AAm), oxoglutaric acid (OG), *N,N*-methylenebisacrylamide (MBAA, Tokyo Chemical Industry), and dimethylformamide (DMF, Sigma–Aldrich) was used as received.

Preparation of Solutions for Electrospinning

Agarose E (1200 mg: monomer), acrylamide (AAm, 900 mg: monomer), oxoglutaric acid (0.0187 g, 1 mol % w.r.t. AAm: photocatalytic initiator), *N,N′*-methylenebisacrylamide solution (0.03 mol % w.r.t. AAm: crosslinker), dimethylformamide (9 mL), and H_2O (1 mL: millipore water) were mixed together, the mixture was heated at 90°C under the constant stirring (300 rpm) in an oil bath for several hours until a clear uniform solution was formed.

Fabrication of Agarose/Polyacrylamide Nanofibers

Above prepared electrospinning solutions or suspensions were transferred to a plastic syringe of 20 mL with a needle inner diameter of 0.58 mm. The needle was connected to a high voltage of positive power supply. The negative terminal was connected an aluminum foil collector. The collector was placed vertically at a horizontal distance of 7.5 cm from the tip. During the electrospinning, the flow rate of the electrospinning solution was fixed at 0.1 mL h^{-1} and the applied voltage was 16–17 kV using NanoNC (ESR200R2D, Korea). Simultaneously photopolymerization reaction performed during the electrospinning procedure was shown in Scheme 1 using UV-lamp (λ: 365 nm, 4w), Dongseo science (UVT series). Acrylamide and *N,N′*-methylenebisacrylamide both the molecules contain amide functional groups, therefore both the molecules undergo simultaneous copolymerization and crosslinking, when irradiated with the UV radiation.

CHARACTERIZATION

Attenuated total reflectance (ATR) Fourier transform infrared (FTIR) spectra of nanofiber sheets were recorded on a Nicolet Nexus FTIR spectrometer (model: iS10, Minnesota).

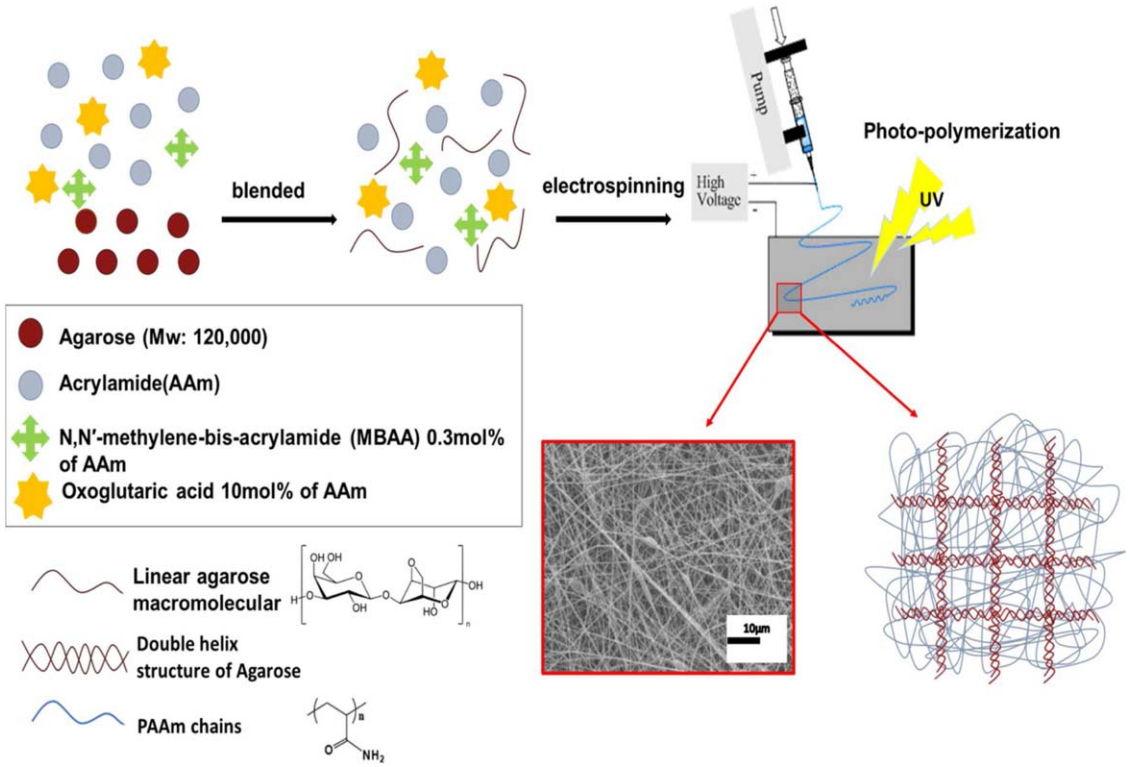

Scheme 1. Preparation of crosslinked DN of agarose/PAAm nanofibers. [Color figure can be viewed in the online issue, which is available at wileyonlinelibrary.com.]

Morphology studies of the nanofiber sheets were carried out with an emission scanning electron microscope (Mini-SEM SNE-4500M). The sample was mounted on a carbon disc with the help of double-sided adhesive tape. Thermogravimetric analysis (TGA) was performed with a thermal analyzer (TGA N-1000 Scinco, Seoul, Korea), Universal at a heating rate of 10°C min^{-1} under a nitrogen atmosphere. The stress–strain measurements were performed of the nanofiber sheets using an universal testing machine (AG-500 KNG, Shimadzu, Tokyo, Japan). The nanofiber sheets were prepared by electrospinning method using NanoNC (ESR200R2D, Korea). The photo polymerization was performed using UV-lamp (λ: 365 nm), Dongseo science (UVT series). Contact angle was measured on PHOENIX-SEO apparatus (Korea).

RESULTS AND DISCUSSION

Fourier Transform Infrared Spectroscopy (FT-IR)

FT-IR spectrum of pure agarose and agarose/AAm was shown in Figure 1. Pure agarose nanofibers sheet were showing peaks at 3342 (O—H stretching), 2904 (—CH_2— stretching), 1633 (bonded H—O—H), 1355, 1157, and 1053 (C—O—C glycosidic linkage), 932 (3,6-anhydro moiety of agarose), and 879 cm^{-1} (β-skeletal bending of basic carbohydrate linkage).[25] Agarose/acrylamide nanofiber sheet showing peaks at 3343 and 3208 cm^{-1} (symmetrical and asymmetrical stretching of the N—H bond), 1662 cm^{-1} (C═O stretching), 1599 cm^{-1} (N—H deformation), 1426 and 1354 cm^{-1} (C—N stretching vibration) 600–800 cm^{-1} (N—H wagging vibration) of the polyacrylamide, 1155 and 1042 cm^{-1} (C—O stretching) of the agarose.[26] In all the prepared nanofiber sheets (Figures 1 and 2), common peaks observed at 3340, 3200, 1660, 1420, 1350, 600–800 cm^{-1} of the polyacrylamide and 1150 and 1040 cm^{-1} of the agarose polymer.

FT-IR spectrum of agarose/PAAm with variation of AAm concentration: 0.0084, 0.0127, 0.0169, and 0.0211 mol % was shown in Figure 2, with increasing the concentration of AAm,

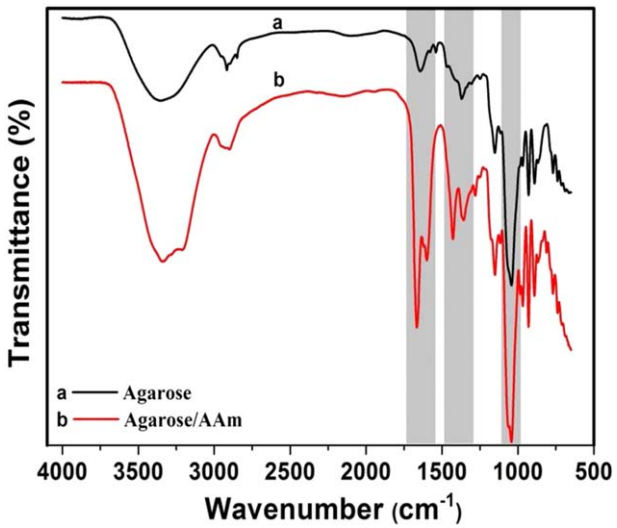

Figure 1. FT-IR spectrum of (a) Agarose-pure and (b) Agarose/AAm nanofiber sheets. [Color figure can be viewed in the online issue, which is available at wileyonlinelibrary.com.]

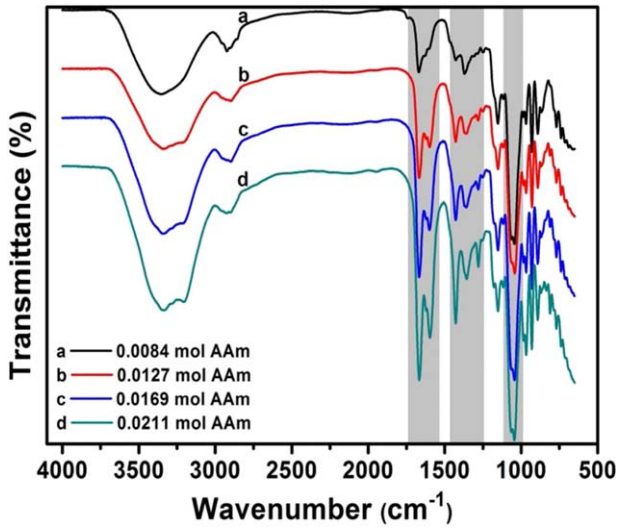

Figure 2. FT-IR spectrum of agarose/PAAm sheets with variation of AAm concentration (a) 0.0084, (b) 0.0127, (c) 0.0169, and (d) 0.0211 mol % AAm. [Color figure can be viewed in the online issue, which is available at wileyonlinelibrary.com.]

the intensity of the peaks at ~1650, 1600, 1426, 1357, and 1278 cm^{-1} was increased supporting for the increasing the polyacrylamide content in the agarose/PAAm electrospun fibrous scaffolds.[26] Similarly, the reverse trend was observed with increasing the concentration of MBAA, the intensity of the peaks at ~1650, 1590, 1420, 1350, and 1270 cm^{-1} was decreased shown in Figure 3, due to the decreasing AAm concentration and increasing the MBAA crosslinking agent concentration in the agarose/PAAm electrospun fibrous scaffolds.

In all the samples strong peaks present at ~1660, 1590, and 1070 were observed in the FT-IR spectra indicating the presence of both agarose and polyacrylamide in the agarose/PAAm nanofiber sheet; it suggests the strong interaction and good compatibility between the two components.[27] From the FT-IR analysis one it confirms the AAm converted into PAAm and formation of the DN with agarose. The -NH_2 groups in polyacrylamide molecules were expected to form hydrogen bonds with the —OH groups in agarose that may create agarose/PAAm complexes. The interactions between agarose and polyacrylamide would be greatly beneficial to the formulation of the blend fibers with a uniform structure as confirmed by their SEM images in Figure 7. Schematic synthesis was shown in Scheme 2.

Thermal Analysis

Thermal analysis of agarose/AAm and crosslinked DN of agarose/PAAm nanofiber sheet were recorded and presented in Figure 4. The pure agarose polymer exhibits two distinct zones of weight loss. The initial weight loss was due to the traces of moisture present in the agarose polymer. The second zone (290–500°C) is due to the rapid degradation of the agarose polymer backbone and almost 100% degradation takes place when temperature reaches 520°C.[28,29] In the case of polyacrylamide, a continuous weight loss starting at the beginning of the heating was observed and at least four thermal degradation stages. The first stage: degradation was due to the loss of moisture, which was present in the polyacrylamide. Second stage: Above 240°C the degradation of polyacrylamide was due to loss of ammonia with the formation of imide group via cyclization. Third stage: The main degradation having a T_{max} at 372°C. Ammonia and water were the only volatile products below 340°C in polyacrylamide. Fourth stage: decomposition of the cyclized product was observed starting from 380°C.[30] The agarose/AAm 100% degradation takes place at 496°C, when the agarose/AAm photopolymerized into crosslinked DN of agarose/PAAm, the resulting agarose/PAAm nanofiber sheet 100% degradation takes place at 653°C, the thermal stability of the agarose/PAAm improved by 157°C (end point). The effect of the AAm concentration on the agarose/PAAm system thermal stability analyzed were shown in Figure 5 (a) 0.0084, (b) 0.0127, (c) 0.0169, and (d) 0.0211 mol % AAm. With increasing the AAm concentration the thermal stability of the agarose/PAAm increases, but in the case of Figure 5(b,c) the thermal stability was almost more or less the same. Effect of the MBAA concentration on the agarose/PAAm system thermal stability analyzed and presented in Figure 6 (a) 0.03, (b) 0.06 and (c) 0.09 mol % MBAA. With increasing the concentration of MBAA the thermal stability of the agarose/PAAm system decreases and Figure 6(b,c) system was showing the almost same thermal stability. All the nanofiber sheet systems were showing thermal stability was close to the pure polyacrylamide.[30]

Morphology Analysis

Morphology analysis of the agarose/AAm and agarose/PAAm nanofiber sheets were recorded and shown in Figure 7. The agarose/AAm [Figure 7(a)] nanofiber sheet show nanofibers formation; when agarose/AAm materials irradiated with photo radiation during electrospinning, AAm undergoes photochemical polymerization in the presence of OG that acts as photochemical initiator resulting in agarose/PAAm formation. The agarose/PAAm [Figure 7(b)] nanofibers were showing the thickness of 250 nm, with uniform morphology. The pure agarose

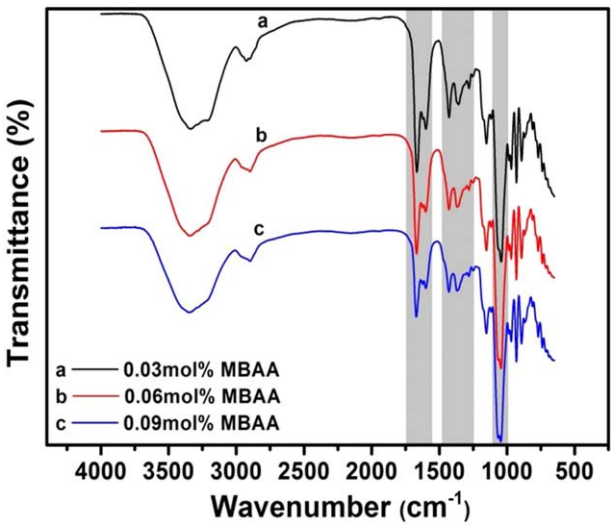

Figure 3. FT-IR spectrum of agarose/PAAm sheets with variation of MBAA concentration (a) 0.03, (b) 0.06, and (c) 0.09 mol % of MBAA. [Color figure can be viewed in the online issue, which is available at wileyonlinelibrary.com.]

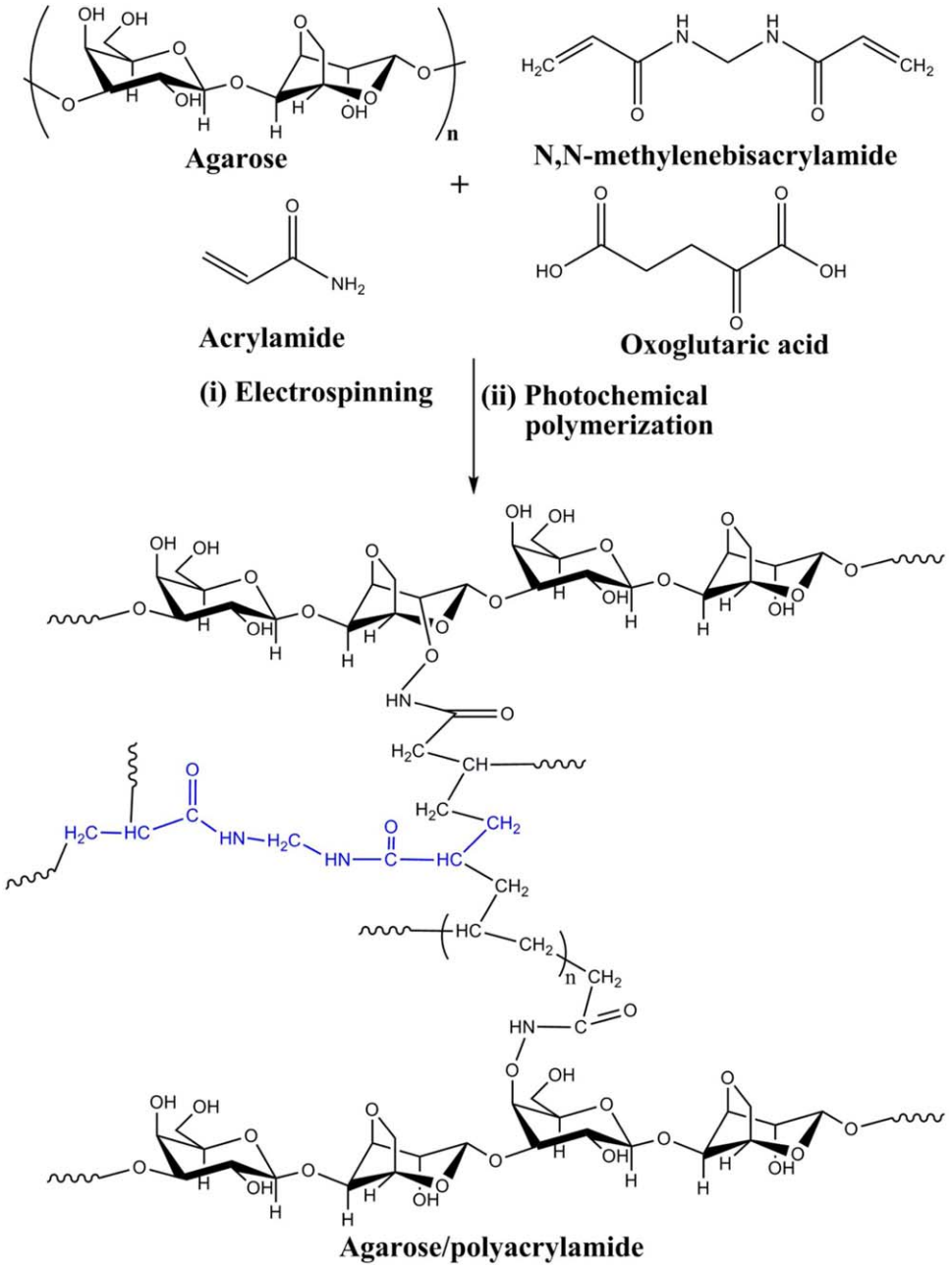

Scheme 2. Synthesis of agarose/PAAm. [Color figure can be viewed in the online issue, which is available at wileyonlinelibrary.com.]

nanofibers sheet was showing the thickness of 365 nm. Therefore with the addition of acrylamide to agarose, the thickness of the agarose/PAAm nanofiber decreases. The effect of AAm concentration on the thickness and shape of the morphology was analyzed and shown in Figure 7(c–f). When the concentration of AAm was 0.0084, 0.0127, 0.0169, and 0.0211 mol %, the nanofiber thickness was found to be 205, 264, 237, and 187 nm, respectively (Figure 7). With the increase in the concentration of the AAm, agarose/PAAm morphology changes from the nanofibers [Figure 7(c,d)] to mixture (nanofibers and agglomerates) [Figure 7(e)] and agglomerates are formed [Figure 7(f)]. Similarly, the effect of the crosslinking agent concentration on the agarose/PAAm system morphology were analyzed and presented in Figure 7. With the increase in the concentration of the MBAA (0.03 to 0.09 mol %), agarose/PAAm present in the nanofibers form and thickness of the agarose/PAAm nanofibers was found to be 264, 353, and 457 nm [Figure 7(g–i)]. Therefore with the increase in the concentration of the crosslinking agent (MBAA), the thickness of the DN of agarose/PAAm nanofibers was increased.

Contact Angle

Contact angle measurements give insight into the surface hydrophilic/hydrophobicity of crosslinked DN of agarose/PAAm system. The contact angle of the agarose/AAm and crosslinked DN of agarose/PAAm system was found to be 45.98° and 35.28°,

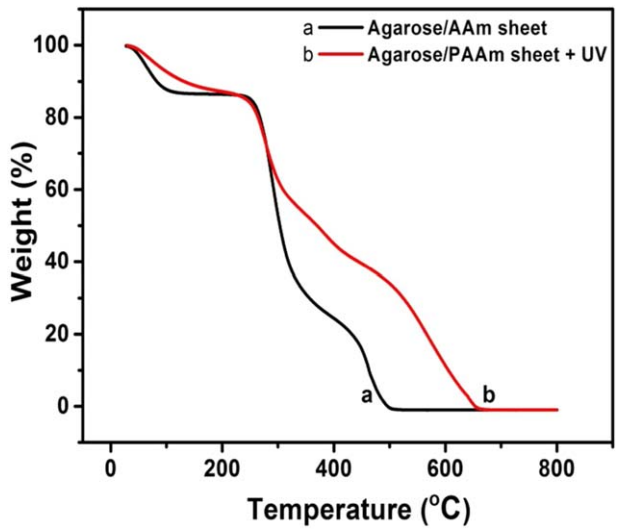

Figure 4. Thermogravimetric analysis of (a) Agarose-pure and (b) Agarose/AAm nanofiber sheets. [Color figure can be viewed in the online issue, which is available at wileyonlinelibrary.com.]

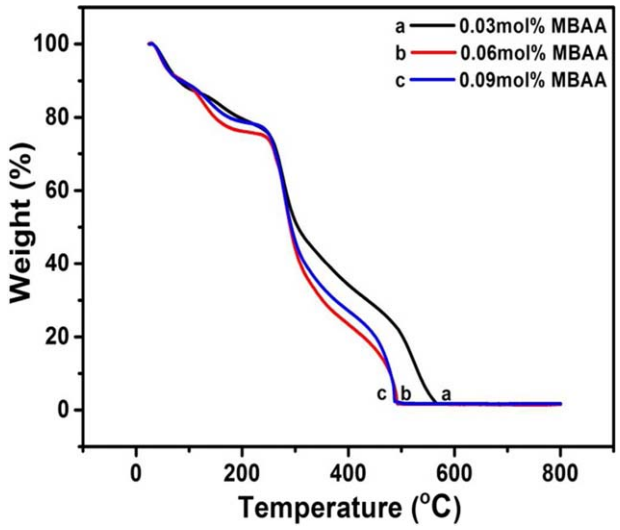

Figure 6. Thermogravimetric analysis of agarose/PAAm nanofiber with variation of MBAA crosslinking density (a) 0.03, (b) 0.06, and (c) 0.09 mol % of MBAA. [Color figure can be viewed in the online issue, which is available at wileyonlinelibrary.com.]

respectively. With the increasing the concentration of the AAm was 0.0084, 0.0127, 0.0169, and 0.0211 mol %, the contact angle of the agarose/PAAm found to be 37.35, 42.62, 44.50, and 47.11°, respectively, indicates the hydrophilicity nature of the crosslinked DN of agarose/PAAm nanofiber sheet decreases. The pure and uniform nanofibers are showing lower contact angle and when nanofibers were converting into the agglomerates (rough surface) contact angle increases.[31] Similarly, the effect of the MBAA concentration on the agarose/PAAm system analyzed, a reverse trend observed compare to the effect of AAm concentration on the agarose/PAAm system, when increasing the concentration of the MBAA, 0.03, 0.06, and 0.09 mol %, the contact angle decreased to 42.62, 38.80, and 35.73° respectively; therefore with the increase in the concentration of the crosslinking agent (MBAA), hydrophilicity nature of the crosslinked DN of agarose/PAAm nanofiber sheet increased. Agarose/PAAm nanofiber sheet showing high contact angle when agarose/PAAm nanofiber was less in thickness and vice versa.[31] The contact angle of the agarose/PAAm nanofiber sheet shown in Figure 8. Pure polyacrylamide was showing contact angle of 23.6.[32] Therefore with addition of agarose polymer to polyacrylamide resulting agarose/PAAm nanofiber sheet contact angle enhances.

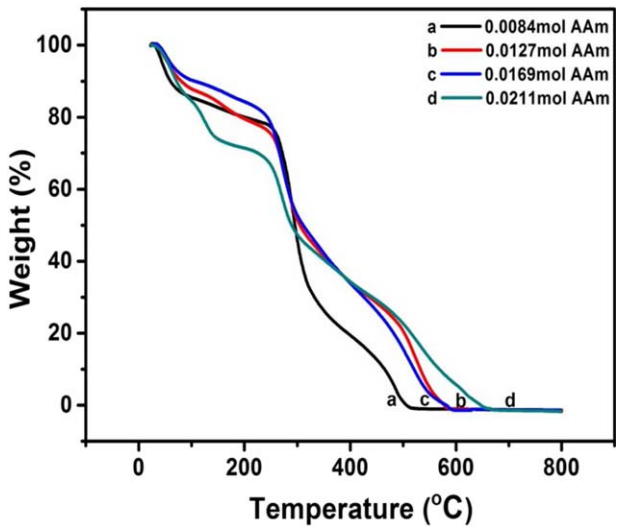

Figure 5. Thermogravimetric analysis of agarose/PAAm sheets with variation of AAm concentration (a) 0.0084, (b) 0.0127, (c) 0.0169, and (d) 0.0211 mol % AAm. [Color figure can be viewed in the online issue, which is available at wileyonlinelibrary.com.]

Mechanical Properties

The mechanical properties of electrospun fibrous scaffolds were determined before and after crosslinking by tensile test. The stress–strain properties of electrospun fibrous scaffolds of agarose, agarose/AAm, and crosslinked DN of agarose/PAAm system were shown in Figure 9. The tensile strength of the agarose, agarose/AAm, and agarose/PAAm system were found to be 6, 7, and 10 MPa, respectively. Pure agarose nanofibers was showing stress 6 MPa, when it is modified with AAm, resulting in agarose/AAm strength improve by 16.66%, when AAm converted into PAAm by the photo polymerization technique in the presence of agarose the strength of the crosslinked DN agarose/PAAm system was improved by 66.66%. The tensile strength of the agarose and DN agarose/PAAm hydrogels was showing around 0.3 and 1.0 MPa respectively.[1] The tensile strength of the DN was much higher than the DN hydrogels. All the tensile properties increased due to the crosslinked DN formation between the agarose and polyacrylamide shown in Schemes 1 and 2.

CONCLUSIONS

We have fabricated the DN of agarose/PAAm nano fibers by simultaneously electrospinning and photo-polymerization method. From the FT-IR analysis it confirms the formation of crosslinked

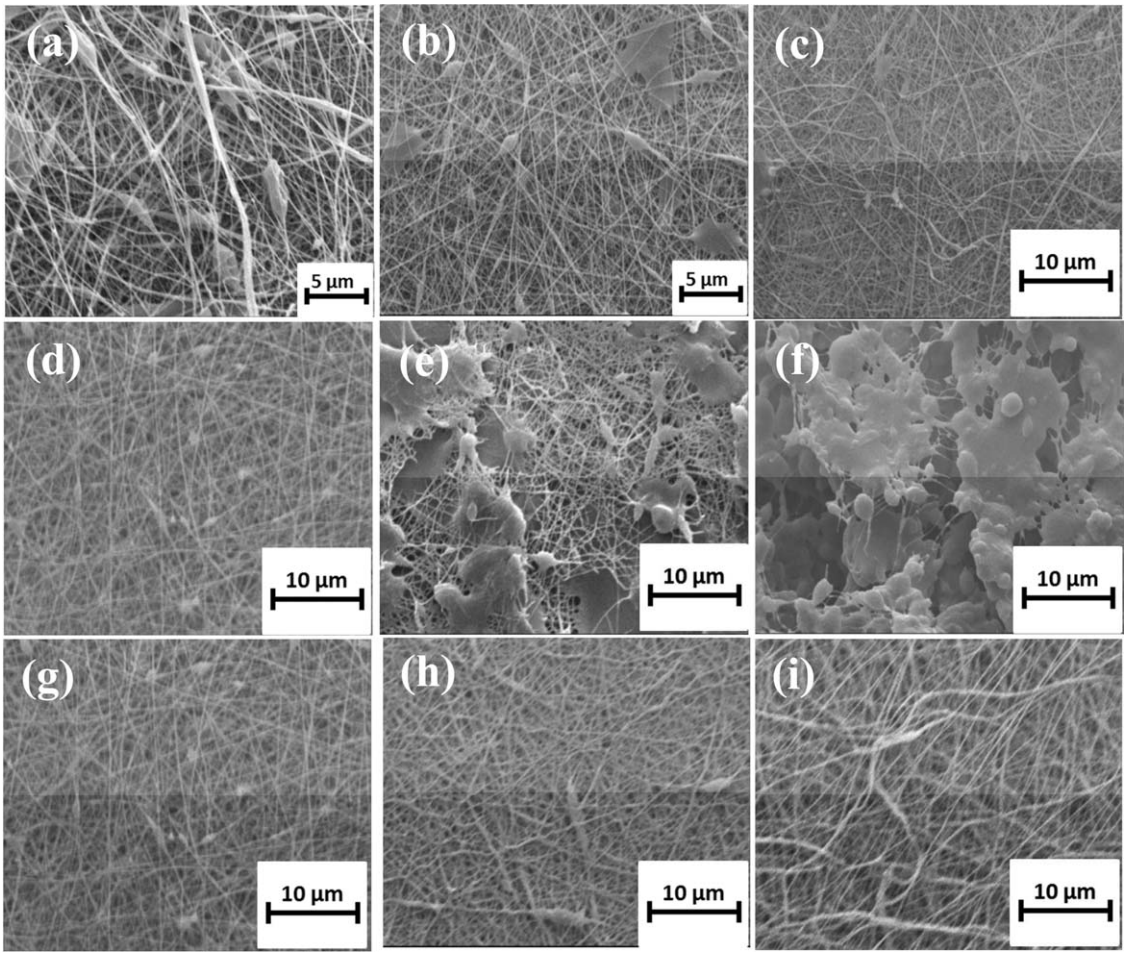

Figure 7. SEM images of (a) agarose/AAm and (b) agarose/PAAm fibers, agarose/PAAm nanofiber sheets with varying concentrations of AAm: (c) 0.0084 mol %, (d) 0.0127 mol %, (e) 0.0169 mol %, and (f) 0.0211 mol % and agarose/PAAm nanofiber sheets with varying concentration of MBAA: (g) 0.03 mol %, (h) 0.06 mol % and (i) 0.09 mol %.

DN of agarose/PAAm. The thermal stability of agarose/PAAm was improved by 157°C compared to the agarose/AAm system and confirming the formation of the agarose/PAAm blended nanofiber sheet. The crosslinked DN of agarose/PAAm system was showing the highly hydrophilic nature. From the SEM analysis, it confirms the uniform agarose/PAAm nanofibers formation and lowest diameter of the nanofibers were found to be around 187 nm. The strength of the electrospun fibrous agarose/PAAm was enhanced by 66.66% compared to the pure agarose. On the basis of these results, we considered that agarose/PAAm fibers could be a potential material in biomedical and bioengineering applications.

Figure 8. Contact angle of agarose/PAAm sheet. [Color figure can be viewed in the online issue, which is available at wileyonlinelibrary.com.]

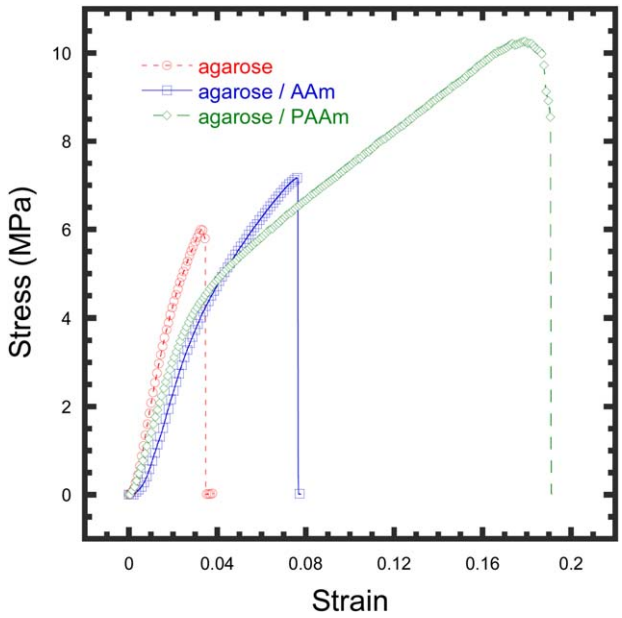

Figure 9. Stress–strain curves agarose, agarose/AAm, and agarose/PAAm nanofiber sheets. [Color figure can be viewed in the online issue, which is available at wileyonlinelibrary.com.]

ACKNOWLEDGMENTS

This work was supported by the National Research Foundation of Korea Grant funded by the Korean Government (MEST) (NRF-2010-0024478) and Hannam University Research Fund in 2015.

REFERENCES

1. Qiang, C.; Lin, Z.; Chao, Z.; Qiuming, W.; Jie, Z. *Adv. Mater.* **2013**, *25*, 4171.
2. Doytcheva, M.; Dotcheva, D.; Stamenova, R.; Orahovats, A.; Tsvetanov, C.; Leder, J. *J. Appl. Polym. Sci.* **1997**, *64*, 2299.
3. Doytcheva, M.; Stamenova, R.; Zvetkov, V.; Tsvetanov, C. B. *Polymer* **1998**, *39*, 6715.
4. Wang, S. F.; Yaszemski, M. J.; Gruetzmacher, J. A.; Lu, L. C. *Polymer* **2008**, *49*, 5692.
5. Wang, S. F.; Yaszemski, M. J.; Knight, A. M.; Gruetzmacher, J. A.; Windebank, A. J.; Lu, L. C. *Acta Biomater.* **2009**, *5*, 1531.
6. Kazanskii, K. S.; Dubrovskii, S. A. *Adv. Polym. Sci.* **1992**, *104*, 97.
7. Maitland, G. C. *Curr. Opin. Colloid Interface Sci.* **2000**, *5*, 301.
8. Calvert, P. *Adv. Mater.* **2009**, *21*, 743.
9. Drury, J. L.; Mooney, D. *J. Biomaterials* **2003**, *24*, 4337.
10. Chauhan, G. S.; Chauhan, S.; Kumar, S.; Kumari, A. *Bioresour. Technol.* **2008**, *99*, 6464.
11. Yi, J. Z.; Zhang, L. M. *Bioresour. Technol.* **2008**, *99*, 2182.
12. Lin, D. C.; Yurke, B.; Langrana, N. A. *J. Biomech. Eng. T ASME* **2004**, *126*, 104.
13. Hynd, M. R.; Turner, J. N.; Shain, W. *J. Biomater. Sci. Polym. Ed.* **2007**, *18*, 1223.
14. Soriano, M. E.; Bourret, E. *Bioresour. Technol.* **2003**, *90*, 329.
15. Xin, X. Z.; Peng, Y. G.; Ce, W. G.; Feng, N. J.; Yan., C. X. *J. Appl. Polym. Sci.* **2006**, *103*, 2759.
16. Santos, C.; Silva, C. J.; Büttel, Z.; Guimarães, R.; Pereira, S. B.; Tamagnini, P.; Zille, A. *Carbohydr. Polym.* **2014**, *99*, 584.
17. Elmira, H. G.; Majid, M.; Masoud, L.; Ali, A.; Ghare, A. *Carbohydr. Polym.* **2014**, *113*, 231.
18. Yinghui, Z.; Ying, Z.; Xiaomian, W.; Lu, W.; Ling, X.; Shicheng, W. *Appl. Surf. Sci.* **2012**, *258*, 8867.
19. Au, T. H.; Beomseok, T.; Jun, S. P. *Carbohydr. Polym.* **2010**, *82*, 472.
20. Richard, M. N. J.; Catherine, N.; Brenda, M.; Andrew, K.; Leslie, P. *Phys. Chem. Earth* **2012**, *50–52*, 243.
21. Chengjun, Z.; Sunyoung, L.; Kerry, D.; Qinglin, W. *J. Hazard. Mater.* **2013**, *263*, 334.
22. Chen, G.; Xu, Y.; Yu, D. G.; Zhang, D. F.; Chattertona, N. P.; White, K. N. *Chem. Commun.* **2015**, *51*, 4623.
23. Wu, Y. H.; Yu, D. G.; Li, X. Y.; Diao, A. H.; Illangakoon, U. E.; Williams, G. R. *J. Mater. Sci.* **2015**, *50*, 3604.
24. Yu, D. G.; Williams, G. R.; Wang, X.; Liu, X. K.; Li, H. L.; Bligh, S. W. A. *RSC Adv.* **2013**, *3*, 4652.
25. Teng, S. H.; Wang, P.; Kim, H. E. *Mater. Lett.* **2009**, *63*, 2510.
26. Zhou, C.; Wu, Q. *Colloids Surf. B* **2011**, *84*, 155.
27. Teng, S.; Shi, J.; Peng, B.; Chen, L. *Compos. Sci. Technol.* **2006**, *66*, 1532.
28. Mihir, D. O.; Ramavatar, M.; Kamalesh, P.; Paul, P.; Siddhanta, A. K. *Carbohydr. Polym.* **2010**, *81*, 878.
29. Mihir, D. O.; Ramavatar, M.; Siddhanta, A. K. *Carbohydr. Polym.* **2012**, *87*, 1971.
30. Durcilene, A. S.; de Paula, R. C. M.; Judith, P. A. F. *Eur. Polym. J.* **2007**, *43*, 2620.
31. Thierry, D.; Frederic, G. *Prog. Polym. Sci.* **2014**, *39*, 656.
32. Shuhui, W.; Shanks, R. A. *J. Appl. Polym. Sci.* **2004**, *93*, 1493.